A versatile polymer-based platform for intracellular delivery of macromolecules

*Michal Kopytynski[1], Siyuan Chen[1], Sandrine Legg[2], Ralph Minter[2], Rongjun Chen[1, *]*

[1] Department of Chemical Engineering, Imperial College London, South Kensington Campus, London, SW7 2AZ, United Kingdom

[2] Department of Antibody Discovery and Protein Engineering, AstraZeneca, Milstein Building, Granta Park, Cambridge CB21 6GH, UK

*Corresponding author:

Email: rongjun.chen@imperial.ac.uk

Keywords: pH-responsive polymer, drug delivery, macromolecular delivery, apoptotic peptide, spheroids

Abstract

The plasma membrane barrier greatly restricts intracellular delivery of macromolecules. Currently available methods suffer from various limitations, including low delivery efficiency, high cytotoxicity or incompatibility with a wider range of macromolecules or cell types. To overcome these issues, stimuli-responsive polymers such as the bio-inspired, pH-responsive poly(L-lysine isophthalamide) grafted with L-phenylalanine at a stoichiometric ratio of 50% (PP50) can be used. In mildly acidic environments, the pseudopeptidic polymer can permeabilize the plasma membrane overcoming the problem of payload entrapment in the endosomes and allowing for efficient intracellular delivery. We demonstrate that PP50 was capable of intracellular delivery by simple co-incubation at pH 6.5 with various macromolecules, including different-sized Dextrans, green fluorescent protein (GFP) and an apoptotic peptide. The delivery process was fast, non-toxic and compatible with multiple cell types, including adherent and suspension cell lines, primary human mesenchymal stem cells,

and cells grown as spheroids. In addition, apoptotic peptide delivery by co-incubation with PP50 was over 3 times more effective than delivery using other common methods, including poly(ethyleneimine) (PEI), cell penetrating peptides (CPPs) and electroporation. Our findings suggest that payload delivery by co-incubation with PP50 is a flexible, controllable method allowing delivery of various payloads to many different cell types *in vitro*.

1. Introduction

Overcoming the barrier posed by the plasma membrane for efficient *in vitro* and *ex vivo* delivery of macromolecules to intracellular compartments remains a challenge [1, 2]. Successful delivery of macromolecular cargo to the cytoplasm and the nucleus would enable a large number of potential applications in fundamental biology and medicine, including the study of protein function without the necessity for DNA transfection, screening of protein and peptide libraries, labelling organelles using intracellular probes as well as delivery of antibodies, production of pluripotent stem cells and cell-based therapy, among others [1, 3-7]. There is therefore an urgent need for a flexible, universal delivery technology.

A 2016 *Nature* review [1] identified seven characteristics of next generation strategies for *in vitro* and *ex vivo* intracellular delivery of materials, which are: (i) good scalability, (ii) applicability for many different cell types, (iii) material independence, (iv) ability to deliver materials to various intracellular target sites, (v) possibility of dosage control, (vi) low cytotoxicity as well as (vii) low cost. In addition, it is desirable that the next generation delivery agent is trigger-sensitive and performs well for delivery of proteins, which, despite advances made in delivery of nucleic acids, remain a problematic cargo [8].

Some of the currently employed intracellular delivery approaches are listed in Table 1 below. Synthetic endosomolytic polymers, such as cationic poly(ethyleneimine) (PEI) or anionic vinyl poly(α-alkylacrylic acid)s, are an improvement on cell penetrating peptides (CPPs) due to the ease of manufacturing, scale up and versatile chemical modifications [23, 24]. A family of anionic, pH-responsive, amphipathic, easy-to-synthesize biopolymers have been designed to mimic naturally occurring fusogenic viral peptides. The optimal PP-polymers are obtained by grafting L-phenylalanine onto the backbone of a pseudopeptidic polymer, poly(L-lysine isophthalamide) (PLP) [20]. Upon protonation of carboxyl groups present on the lysine and phenylalanine residues, the biomimetic polymers can undergo a pH-dependent coil-to-globule conformation change, which as a result leads to reversible permeabilization of biological membranes [20,25]. The membrane-permeabilizing ability of PP-polymers can be manipulated by controlling the degree of grafting with L-phenylalanine, ensuring that electrostatic repulsion between the negatively charged polymers and the negatively charged cell membrane can be outweighed by hydrophobic interaction [25, 26]. PP-polymers possess advantages over other types of anionic polymers by incorporating biodegradable amide bonds that avoid the disadvantages of non-biodegradable alternatives such as vinyl-based polycarboxylates, which are limited in size by the renal-exclusion limit. PP-polymers cause low cytotoxicity and reduce the risk of unwanted interaction with negatively charged serum proteins due to their anionic charge [26, 27], which are two advantages compared to cationic polymers such as PEI. Among other applications, PP-polymers have been successfully used for *in vitro* and *in vivo* delivery of siRNA by conjugation [28] and *in vitro* delivery of an apoptotic protein by complexation [29] to their intracellular sites of action following endosomal escape.

PP50, one of the polymers from the PP-family, is obtained by grafting PLP with L-phenylalanine at a stoichiometric ratio of 50 mol% relative to the pendant carboxylic acid groups [30]. PP50 has been previously demonstrated to deliver small-molecule trehalose

through simple mixing to human erythrocytes and osteosarcoma cells at a mildly acidic extracellular pH for cryopreservation applications, while causing minimal cytotoxicity [31, 32]. In this paper, we explore the possibility of greatly expanding the scope of using PP50 as a bio-inspired, next generation delivery agent, compatible with many model and functional macromolecular payloads and enabling cytoplasmic delivery to a wide range of cell types.

2. Results

2.1. Delivery method

We hypothesize that treatment of nucleated mammalian cells with a mixture of PP50 and a fluorescent macromolecular payload results in payload delivery to the cytoplasm, and that this effect is enhanced by mildly acidic extracellular environment due to the pH-triggered membrane permeabilization by PP50. To test this, we used fluorescein isothiocyanate–Dextran (FITC-Dextran) as the model payload. The structure and NMR spectrum of PP50 used herein are shown in Figure S1.

To initially investigate PP50-mediated intracellular delivery, HeLa cells were co-incubated with a 150 kDa FITC-Dextran payload (the same molecular weight as an IgG antibody) at pH 6.5 and pH 7.4 in the presence and absence of the polymer. Confocal microscopy images **(Figure 1a)** taken following a 30 min treatment show that PP50 successfully facilitated intracellular delivery of the macromolecular payload, compared to the corresponding negative controls in the absence of PP50. The green diffuse staining throughout the cytoplasm was uniform and not co-localized with the endosomal-lysosomal stain Lysotracker (red channel) (**Figure 1a** and **1b**). This pattern suggests that the problem of endosomal entrapment was avoided [33]. Furthermore, the level of FITC-Dextran delivery at pH 6.5 was notably higher than that at pH 7.4. In addition, we observed localization of FITC-Dextran inside the nuclei (**Figure 1a** and **1b**), which was further confirmed using Z-stack three-dimensional (3D)

projection showing co-localization of the green fluorescence with the blue-fluorescent DNA dye Hoechst (**Figure 1c**).

The interaction between PP50 and FITC-Dextran was examined using dynamic light scattering (DLS), by comparing the hydrodynamic size distribution and polydispersity index (PDI) of the mixture of PP50 and FITC-Dextran in aqueous solution to those of the two components alone. As shown in Figure S2, both PP50 and FITC-Dextran demonstrated a single size distribution, with an average hydrodynamic size of 41.9 ± 0.4 nm (PDI = 0.203 ± 0.005) and 94.9 ± 1.0 nm (PDI = 0.268 ± 0.005), respectively. As comparison, the average size of the particles in the mixture of those two components was equal to 55.0 ± 0.24 nm (PDI = 0.456 ± 0.006) with two distinct peaks around 30 and 105 nm, indicative of limited interaction between PP50 and FITC-Dextran subsequent to mixing. This suggests that the two components were present in the solution with no obvious formation of complexes and PP50 permeabilized the phospholipid membrane before cytoplasmic localization of the delivered substances.

2.2. Delivery characterization

The amount of payload delivered intracellularly is a function of parameters such as treatment time, extracellular pH and polymer concentration. These were studied to assess the flexibility of this delivery method and were quantified using flow cytometry.

Time-dependent intracellular delivery of FITC-Dextran (150 kDa) at pH 6.5 was investigated, demonstrating that the process was most efficient within the first 1 h (**Figure 2a**). The first detectable signal appeared between 5-15 min of treatment (Figure S3), which suggests that the underlying delivery mechanism was rapid. The intensity of the fluorescent signal was further increased by extending the treatment period up to 3 h, with the fluorescent intensity of the

cells treated with the polymer being 6.2 times brighter compared to the polymer-free control samples.

In addition, we demonstrated that that the intracellular amount of the desired payloads could be modulated by changing the payload concentration in the extracellular environment, which can be done independently of polymer concentration (Figure S4). Furthermore, we observed that treatment of HeLa cells with a low concentration of PP50 (50 μg mL^{-1}) resulted in a substantial intracellular loading of the 150 kDa FITC-Dextran (Figure S5). Cell fluorescence was further enhanced by increasing the polymer concentration, but reached a plateau at the concentration of approximately 1 mg mL^{-1}, suggesting that a higher PP50 concentration was not required for efficient delivery under the studied conditions. The efficiency of the delivery process was also further enhanced by lowering the extracellular pH values to pH 5.5-6.0 (**Figure 2b**). This pH-responsive effect allows for additional flexibility in designing protocols in which mildly acidic pH can be used as a trigger to greatly enhance intracellular delivery.

PP-polymers have been previously reported to be non-cytotoxic to mammalian cells at workable concentrations [25, 34] and PP50 was shown to be well tolerated by HeLa cells after a prolonged period of 24 h treatment (Figure S6). In addition, we investigated the cytotoxicity of the delivery process of 150 kDa Dextran to HeLa cells. By varying polymer concentration, we found that delivery of 150 kDa Dextran (10 μM) resulted in negligible cell cytotoxicity at both pH 6.5 and 7.4, including at the maximal PP50 concentration tested of 2 mg mL^{-1} (**Figure 2c**). After extended treatment to 3 h, only a slight decrease in cell survival to 93% and 87% for pH 7.4 and pH 6.5, respectively, was observed (**Figure 2d**).

2.3. Delivery to different cell lines

PP50-mediated delivery of 150 kDa FITC-Dextran was tested in 9 different cell types *in vitro* to illustrate the wide applicability of this technique. We used a selection of common human and animal cell types such as human cervical cancer (HeLa), human lung carcinoma (A549), human uterus sarcoma (MES-SA) and doxorubicin (a widely used chemotherapeutic drug)-resistant MES-SA (MES-SA/Dx5), murine osteoblastic cells (MC 3t3), Chinese hamster ovarian cells (CHO), human B lymphocytes (SU-DHL-8), murine macrophage/monocytes (RAW 264.7) as well as human mesenchymal stem cells (hMSCs). We found that in all cases, the 150 kDa FITC-Dextran was successfully delivered to the cytoplasm when incubated with PP50 at pH 6.5 (**Figure 3**). Spots in the green channel, indicating a level of endosomal entrapment, were observed only in the case of CHO cells, however, that did not prevent successful delivery to the cytoplasm and the nucleus. In addition, the delivery process was well tolerated by all the cells used (Figure S7).

2.4. Delivery to multicellular spheroids

3D multicellular spheroids are often used as models of tumor and tissue environments as they are more representative of the real complexity and heterogeneity of these systems compared to 2D cell monolayers [35]. Thus, efficient delivery of macromolecules to multicellular spheroids could be of great interest in the fields of fundamental and tumor biology.

To assess payload delivery to spheroids using PP50, we co-incubated 2-day old A549 spheroids with 150 kDa FITC-Dextran (10 μM) and PP50 (0.5 mg mL^{-1}) and analyzed the samples using confocal microscopy (**Figure 4**). Successful cytoplasmic delivery of Dextran was observed in the samples where the spheroids were co-incubated with PP50 at pH 6.5, the cells clearly visible in the green channel. A low level of fluorescence was observed in the polymer negative controls. Since 150 kDa FITC-Dextran alone was not shown to escape

endosomes in the previous experiments, the signal possibly came from the payload trapped in the endosomes as well as in the intercellular space of the spheroids, which is consistent with a pattern reported previously [27]. Furthermore, the relatively small number of cells stained with propidium iodide (PI) in both polymer-free and polymer-containing samples is consistent with other observations regarding cell viability in A549 spheroid [36] and further illustrates that the delivery process using PP50 had negligible cytotoxicity.

2.5. Delivery of different-sized model payloads

To further assess the flexibility of this delivery method, we treated HeLa cells with PP50 and FITC-Dextran with various molecular sizes of 10, 70, 150 and 500 kDa at pH 6.5. These Dextrans represent a wide size range corresponding to that of peptides, proteins, antibodies, RNAs and plasmids.

We found that after a short treatment of 30 min we could obtain a cytoplasmic and nuclear fluorescent signal which was sufficiently strong for detection (**Figure 5a**). We did not observe any punctuate staining in the green channel, suggesting there was little endosomal entrapment occurring. This was further confirmed by flow cytometry, showing an average 4.2-fold stronger fluorescent signal in cells delivered with 10, 70, 150 and 500 kDa payloads compared to the corresponding polymer-free control samples (**Figure 5b**, $***p \leq 0.001$). In addition, the delivery efficiency might be conversely proportional to the Dextran size. We also demonstrated intracellular delivery of green fluorescent protein (GFP, Mw = 26.9 kDa) resulting in a diffuse signal in the cytoplasm and the nucleus after 1 h co-treatment with PP50 at pH 6.5 (**Figure 5c**).

2.6. Delivery of apoptotic peptide

The ability to deliver functional payloads is another major requirement for a successful delivery agent and must be investigated. We used Bim, a pro-apoptotic peptide which has been reported to play a key role in the regulation of apoptosis through interacting with other B-cell lymphoma 2 (Bcl-2) family proteins [37]. Upon interaction with the BH3 region of Bim, the antiapoptotic members of the Bcl-2 protein family are inactivated, leading to initiation of the apoptotic pathway via the Caspase 9 route [37].

We tested delivery of Bim to A549 cells by co-incubation with PP50 at physiological and mildly acidic pH. The apoptotic effect was assessed by detection of Caspase 3/7 activation, known as the apoptosis executioners, as well as the AlamarBlue assay or CellTiter-Glo 2.0 assay, to quantify cell viability post-treatment. We found that Bim co-incubated with PP50 at pH 6.5, but not at pH 7.4, induced a noticeable Caspase 3/7 activation response (**Figure 6a**, ***$p \leq 0.001$), which was in line with the other intracellular delivery results reported herein. In addition, the apoptotic response was not induced by Bim or PP50 on its own, or inactive, scrambled Bim (scrBim) co-incubated with PP50, but was seen when the cells were incubated with the membrane-permeable, small-molecule Bcl-2 inhibitor, ABT-737 [38]. Furthermore, the cell survival rate after a further incubation period of 24 h confirmed the successful triggering of apoptosis (**Figure 6b**).

In addition, we performed dose titration studies of Bim using a fixed PP50 concentration. We found that an initial Caspase 3/7 response can be seen at the extracellular Bim concentration of 5 μM (**Figure 6c**, *$0.01 < p \leq 0.05$). This is in line with results reported for delivery of trans-activating transcriptional activator (Tat)-Bim, where the apoptosis response was observed after treatment with 2-5 μM of these conjugates, depending on the cell type used [39]. We also analyzed intracellular delivery of Bim and scrBim fluorescently labelled with sulfocyanine7 (Cy7) to A549 cells using flow cytometry and observed that co-incubation with

PP50 caused a 5.5-fold increase in median cell fluorescence compared to polymer-negative samples for both peptides (**Figure 6d**). The difference in fluorescence intensity between cells only and the cells incubated with the peptide at a relatively high extracellular concentration might be explained by non-specific peptide binding to the cell surface and endosomal entrapment. The considerable increase in cell fluorescence in the PP50-containing samples suggests that the polymer substantially enhanced the cytoplasmic delivery of the peptide.

Finally, delivery of the Cy7-labelled Bim and scrBim (15 μM) using PP50 was compared to delivery using a panel of different intracellular delivery methods (**Figure 6e**). This included co-incubation with PLP, the parent polymer of PP50, 0.6 kDa branched and 25 kDa linear PEI [40, 41], melittin [42], Tat peptide [43], penetratin [44], PULSin® [45], BioPORTER® [46] as well as via electroporation. Delivery of Bim using PP50 was the most potent, leading to 21 ± 1.5% cell survival compared to 90 ± 3.3% survival in the samples co-incubated with PP50 and scrBim (***$p \leq 0.001$). The 25 kDa linear PEI, achieved 65% cell survival, but this effect could be caused by cytotoxicity of this polymer as the cell survival of cells co-incubated with PEI and scrBim was also low. This comparison suggests that PP50 is a more efficient delivery agent than commonly used CPPs and PEI when using the simple co-incubation strategy, and outperforms two commercially available protein delivery kits, PULSin® and BioPORTER®, as well as electroporation.

3. Discussion

Here, we investigate the use of a pH-responsive, membrane-permeabilizing polymer PP50 for the intracellular delivery of different payloads. By co-incubating the polymer with different macromolecular model and functional cargos as well as 9 different cell types we show that PP50 is a versatile and efficient delivery agent with a quick and easy protocol.

We demonstrate that transient mildly acidic extracellular pH during the treatment greatly enhances delivery efficiency and allows for a level of control in potential future experimental design. Fluorescently labelled PP50 applied to human osteosarcoma cells at neutral pH was shown to internalize mostly via clathrin- and caveolin-mediated endocytosis as well as macropinocytosis [47]. Other researchers have reported that endocytosed macromolecules are trafficked from early endosomes to late endosomes and then lysosomes within several hours [23]. However, we observed rapid intracellular delivery after only 5-15 min of co-incubation of cells with PP50 and macromolecular payloads at mildly acidic extracellular pH (**Figure 2a** and Figure S3) and it was payload size dependent (**Figure 5**). This could be attributed to the altered delivery mechanism with extracellular acidity. Lynch *et al*. found that binding of PP50 on the erythrocyte membrane at mildly acidic extracellular pH led to localized membrane thinning of 35-40% of the total membrane thickness, and could explain the observed intracellular loading of trehalose [31]. Considering that erythrocytes do not undergo phagocytosis or endocytosis [48], it is believed that PP50 can cause intracellular delivery through direct membrane permeation due to extracellular acidity induced membrane thinning. In this paper, the membrane permeation process was shown to be tunable for various model and functional macromolecular payloads of different sizes and chemical properties in a wide range of cell lines and multicellular spheroids (**Figures 3-6**). We found that there was no obvious formation of complexes between PP50 and the delivered substances (Figure S2), suggesting that PP50 permeabilized the membrane followed by the cross-membrane transport of macromolecular payloads. Another possibility is that PP50 might bind to the plasma membrane and is taken-up via endosomal pathways in its membrane-active state, leading to quick destabilization of early endosomes and leakage.

Based on the results herein, we propose PP50 as a candidate which meets many of the criteria of a next generation delivery agent [1]. We demonstrated that PP50 could deliver different-sized payloads varying in terms of their chemical and physical properties, such as fluorescent Dextran, proteins and peptides. Particularly, PP50-mediated delivery performed better than a number of other commonly used delivery techniques for delivery of the apoptotic peptide Bim. Further work is needed to assess PP50-mediated delivery of nucleic acids by co-incubation, however, delivery of siRNA has already been demonstrated for other PP-polymer by conjugation [28]. In addition, we showed that PP50 could deliver macromolecular payloads to a variety of different cell types, including delivery to hard-to-transfect hMSCs. We predict that PP50-mediated delivery is compatible with many more cell types. In addition, there is growing interest in the use of exosomes and extracellular vesicles (EVs) for drug delivery applications. Based on the cross-membrane delivery results shown herein, we believe that PP50 could be used to load desired payloads across the vesicular membrane into EVs or EV-producing cells for drug delivery applications. We also demonstrated that PP50-mediated delivery worked with adherent and suspension cells, as well as 3D multicellular spheroids which allow the study of cells in a more physiological state.

Molecules delivered using PP50 were shown to retain their functional abilities. Since the delivery process relies on simple co-incubation rather than conjugation, the risk of disrupting the payloads' structure and function is low. In addition, we noticed localization of the fluorescent Dextrans inside the nuclei. It was previously reported that 70 kDa fluorescent Dextran delivered to the cytoplasm using a CPP did not penetrate the nuclear envelope due to size restrictions, as it is generally believed that the nuclear pores greatly limit transport of molecules larger than 50 kDa [49-51]. We were therefore surprised to observe that all the different-sized FITC-Dextrans (10, 70, 150 and 500 kDa) used were localized inside the nuclei of all the 9 different cell types tested, which could suggest that PP50 allows for

permeabilization or transport across the nuclear envelope. The precise mechanism by which this occurs is not yet understood. If confirmed, this could enable using PP50 for cell modification applications by facilitating the delivery of the CRISPR/Cas9 system [52].

In conclusion, we have shown that PP50-mediated delivery is a versatile platform technology, compatible with payloads of different sizes and chemical properties and compatible with different mammalian cell types grown in 2D and 3D formats. It possesses several advantages over using other chemical or physical delivery methods.

4. Experimental Section

Materials

FITC-Dextran of different sizes (average Mw = 10, 70, 150 and 500 kDa, respectively), Dulbecco's modified Eagle's medium (DMEM), Roswell Park Memorial Institute (RPMI), foetal bovine serum (FBS), alpha-modified Minimum Essential Medium (alpha-MEM), McCoy's 5A culture medium, melittin (GIGAVLKVLTTGLPALISWIKRKRQQ), Tat (YGRKKRRQRRR), BioPORTER® and penicillin were purchased from Sigma Aldrich (Dorset, UK). AlamarBlue assay kit, PEI 0.6 kDa (branched) and 25 kDa (linear) were purchased from Fisher Scientific (Loughborough, UK). Anhydrous ethanol, acetone, hydrochloric acid, sodium hydroxide and PULSin® were obtained from VWR (Lutterworth, UK). Caspase-Glo® 3/7 assay and CellTiter-Glo® 2.0 assay kits were purchased from Promega (Southampton, UK). Penetratin (RQIKIWFQNRRMKWKKGG) was purchased from Tebu-Bio (Peterborough, UK). Electroporation kit (Cell Line Nucleofector® Kit T) was purchased from Lonza (Slough, UK). Cy7-labelled Bim ([Sulfocyanine7]-RPEI-W-IAQELRRIGDEFNAYYAR-Ahx-Cys-amide) and scrBim ([Sulfocyanine7]-DLERRGIANFEQAI-W-RAYYIEPR-Ahx-Cys-amide) were purchased from Cambridge Research Biochemicals (Billingham, UK). PP50 polymer (M_w = 46 kDa, polydispersity = 1.99) was synthesized in-house according to the method published by Chen *et al.* and its structure and NMR spectrum are shown in Figure S1 [20].

Cell culture

HeLa, A549 and RAW 264.7 cells were grown in DMEM. CHO cells were grown in DMEM supplemented with 1% non-essential amino acids. SU-DHL-8 suspension cells were grown in RPMI medium. hMSC and MC 3t3 cells were grown in alpha-MEM. MES-SA and MES-SA/Dx5 cells were grown in McCoy's 5A culture medium. All the culture media were also supplemented with 10% (v/v) FBS, 100 Units mL^{-1} penicillin and 100 µg mL^{-1} streptomycin and maintained in a humidified incubator at 37 °C with 5% CO_2.

Payload delivery and confocal microscopy imaging

Different-sized FITC-Dextans were used as models of similarly-sized functional macromolecules to study PP50-faciliated intracellular delivery. Appropriate cell types were seeded in collagen-coated, glass-bottom dishes (35 mm, MatTek, USA) at 1 x 10^5 cells per dish and cultured in an incubator with 5% CO_2 at 37 °C for 24 h. The cells were then treated with magnesium and calcium-containing Dulbecco's Phosphate-Buffered Saline (D-PBS, Sigma Aldrich, UK) with a specific concentration of PP50 and FITC-Dextran, whose pH was adjusted to 6.5 or 7.4 and sterile-filtered using 0.22 µm syringe filters. After treatment, the cells were washed with D-PBS and then stained with LysoTracker® red DND-99 (50 nM) and Hoechst 33342 (1 µg mL^{-1}). 1 mL of DMEM was added to each dish and the cells were analyzed using an LSM-510 laser scanning inverted confocal microscope (Zeiss, Germany). Hoechst, FITC-Dextran and LysoTracker® were excited at 405, 488 and 561 nm, respectively. The images were analyzed using ImageJ 1.51n.

Flow cytometry

1 mL of HeLa cells (3 x 10^5 cells mL^{-1}) were cultured in 6-well plates for 24 h followed by treatment with a pH-adjusted D-PBS solution containing a desired concentration of PP50 and FITC-Dextran. Following the treatment, the cells were washed with D-PBS. After cell

detachment using 0.5 mL of Trypsin-EDTA (or EDTA in case of MES-SA and MES-SA/Dx5 cells and cell scraping in case of RAW 264.7 cells), 0.5 mL of serum-free growth medium was added to each well and the samples were centrifuged in 2 mL Eppendorf tubes for 5 min at 1000 rpm. The supernatant was discarded and replaced with 0.5 mL of serum-free medium. The samples were filtered using Flowmi™ cell strainers (40 μm) and analyzed in 5 mL Falcon plastic tubes using a BD LSRFortessa cytometer. The samples were excited at 488 nm and the emission was collected in the 570 - 585/42 nm band. The results were analyzed using FlowJo v10.

AlamarBlue assay

Cells were seeded in black, flat, transparent-bottom 96-well plates (Corning, USA) at 1 x 10^4 cells per well in 0.1 mL culture medium and incubated for 24 h. The spent medium was replaced with sterile-filtered D-PBS containing PP50 or PP50 mixed with Dextran and incubated for a specific period of time. The polymer solutions were replaced with DMEM containing the 10% (v/v) AlamarBlue reagent and further incubated for 4 h, as per the manufacturer's protocol. The fluorescence was measured using a spectrofluorometer (GloMax®-Multi Detection System, Promega) at the emission wavelength of 580-640 nm and the excitation wavelength of 525 nm. The cytotoxic effect was determined by comparison to an untreated control cell sample.

Spheroids

A549 cells were seeded at 2.5 x 10^3 cells per well in DMEM in Corning® 96-well ultra-low attachment spheroid microplates and cultured in an incubator (5% CO_2 at 37 °C) for 2 days. The spheroids which formed at the bottom of the wells were treated with FITC-Dextran (10 μM) at pH 6.5 and 7.4 for 2 h with or without PP50 (0.5 mg mL^{-1}). The spheroids were subsequently washed 3 times by submerging in 10 mL of D-PBS and stained with propidium

iodide (1 μg mL^{-1}). They were then characterized using Z-stack imaging with an LSM-510 laser scanning confocal microscope. The image analysis was performed using Volocity Version 6.3.0.

Peptide delivery and Caspase 3/7 assay

A549 cells were seeded in white, flat-bottom, opaque 96-well plates (Corning, USA) at 5 x 10^3 cells per well in 0.1 mL culture medium and incubated for 24 h. The spent medium was replaced with sterile-filtered D-PBS containing PP50 and Bim and incubated for 3 h. The solutions were replaced with DMEM and further incubated for 4 h. After that the growth medium was removed and replaced with 20 μL of serum-free DMEM. 20 μL of Caspase-Glo® 3/7 Assay reagent was added to each of the wells and incubated in a plate shaker for 1 h at room temperature. The luminescence was measured using a spectrofluorometer (GloMax®-Multi Detection System, Promega). The cytotoxic effect was determined by comparison to appropriate control samples. Corresponding AlamarBlue assays were performed as described above.

Delivery method comparison

A549 cells were cultured in 96-well plates (Corning, USA) at 2 x 10^4 cells per well. 15 μM Bim-Cy7 and scrBim-Cy7 were added to the cells mixed with the following delivery agents: PP50 (22 μM), PLP (29 μM), PEI 0.6 kDa (1.7 mM), PEI 25 kDa (2 μM), Melittin (1 μM), Tat (20 μM) and Penetratin (20 μM). These concentrations were determined according to literature and experimental optimization [43, 44, 53]. Peptide delivery using BioPORTER®, PULSin® and electroporation was performed using manufacturer's instructions. Treatment time was equal to 4 h in either D-PBS pH 6.5 (PP50 and PLP) or serum-free DMEM (PEI, Melittin, Tat, Penetratin, Pulsin, Bioporter). Cell survival was assessed using CellTiter-Glo®

2.0 by adding 40 µL of the assay reagent to each of the wells 24 h post-treatment, and the luminescence was analyzed using an Envision 2100-series plate reader and compared to appropriate controls containing untreated cells.

Statistical analysis

The quantitative data were expressed as mean ± standard deviations. The number of replicates for each experiment has been specified in the captions of Figures 2, 5 and 6, respectively. In flow cytometry, the reported values are based on 10,000 events for each sample. A two tailed Student's t test was performed to evaluate the statistical significance of difference. A value of $P < 0.05$ was considered to be statistically significant and is shown as follows: $*0.01 < p \leq 0.05$; $**0.001 < p \leq 0.01$; and $***p \leq 0.001$. Analysis of quantitative data was performed in GraphPad Prism 8 and Microsoft Excel. The presented confocal microscopy images are representative of the wider cell population in the given experimental samples.

Supporting Information

Supporting Information is available from the Wiley Online Library or from the author.

Acknowledgements

The authors thank the Biotechnology and Biological Sciences Research Council (BBSRC, UK) and AstraZeneca (UK) for funding this research. The authors also thank GlaxoSmithKline plc for the financial support through the Engineered Medicines Laboratory (EML), as well as Professor Molly Stevens and Dr Spencer Crowder (both Imperial College London) for providing hMSCs. The authors would like to thank Department of Chemical Engineering at Imperial College London and AstraZeneca for access to research facilities, and

the Facility for Imaging by Light Microscopy (FILM) at Imperial College London for access to the Zeiss LSM-510 inverted laser scanning confocal microscope.

Author contributions: R.C. supervised and coordinated research; R.C., R.M., S.L., and M.K. designed research; M.K. performed research; M.K., R.C. and S.C. analyzed data; and M.K., R.C., R.M., and S.L. wrote the paper.

The authors declare no conflict of interest.

Received: ((will be filled in by the editorial staff))
Revised: ((will be filled in by the editorial staff))
Published online: ((will be filled in by the editorial staff))

References

[1] M. P. Stewart, A. Sharei, X. Ding, G. Sahay, R. Langer, K. F. Jensen, *Nature* **2016**, 538, 183.
[2] I. A. Khalil, K. Kogure, H. Akita, H. Harashima, *Pharmacological reviews* **2006**, 58, 32.
[3] A. Kollmannsperger, A. Sharei, A. Raulf, M. Heilemann, R. Langer, K. F. Jensen, R. Wieneke, R. Tampé, *Nature Communications* **2016**, 7, 10372.
[4] J.-W. Yoo, D. J. Irvine, D. E. Discher, S. Mitragotri, *Nat Rev Drug Discov* **2011**, 10, 521.
[5] L. Rajendran, H.-J. Knolker, K. Simons, *Nat Rev Drug Discov* **2010**, 9, 29.
[6] A. L. Marschall, C. Zhang, A. Frenzel, T. Schirrmann, M. Hust, F. Perez, S. Dubel, *MAbs* **2014**, 6, 943.
[7] D. Kim, C. H. Kim, J. I. Moon, Y. G. Chung, M. Y. Chang, B. S. Han, S. Ko, E. Yang, K. Y. Cha, R. Lanza, K. S. Kim, *Cell stem cell* **2009**, 4, 472.
[8] S. Guillard, R. R. Minter, R. H. Jackson, *Trends in Biotechnology* **2015**, 33, 163.
[9] J. L. Young, D. A. Dean, *Advances in genetics* **2015**, 89, 49.
[10] Y. Zhang, L. C. Yu, *BioEssays: news and reviews in molecular, cellular and developmental biology* **2008**, 30, 606.

[11] A. Sharei, J. Zoldan, A. Adamo, W. Y. Sim, N. Cho, E. Jackson, S. Mao, S. Schneider, M.-J. Han, A. Lytton-Jean, P. A. Basto, S. Jhunjhunwala, J. Lee, D. A. Heller, J. W. Kang, G. C. Hartoularos, K.-S. Kim, D. G. Anderson, R. Langer, K. F. Jensen, *Proceedings of the National Academy of Sciences* **2013**, 110, 2082.
[12] M. T. Saung, A. Sharei, V. A. Adalsteinsson, N. Cho, T. Kamath, C. Ruiz, J. Kirkpatrick, N. Patel, M. Mino-Kenudson, S. P. Thayer, R. Langer, K. F. Jensen, A. S. Liss, J. C. Love, *Small (Weinheim an der Bergstrasse, Germany)* **2016**, DOI: 10.1002/smll.201601155.
[13] N. Yim, S. W. Ryu, K. Choi, K. R. Lee, S. Lee, H. Choi, J. Kim, M. R. Shaker, W. Sun, J. H. Park, D. Kim, W. D. Heo, C. Choi, *Nat Commun* **2016**, 7, 12277.
[14] V. P. Torchilin, *Nat Rev Drug Discov* **2005**, 4, 145.
[15] F. Heitz, M. C. Morris, G. Divita, *British journal of pharmacology* **2009**, 157, 195.
[16] D. Weerakkody, A. Moshnikova, M. S. Thakur, V. Moshnikova, J. Daniels, D. M. Engelman, O. A. Andreev, Y. K. Reshetnyak, *Proceedings of the National Academy of Sciences* **2013**, 110, 5834.
[17] D. Zhang, J. Wang, D. Xu, *Journal of Controlled Release* **2016**, 229, 130.
[18] A. Pikabea, E. Villar-Álvarez, J. Forcada, P. Taboada, *Journal of Molecular Liquids* **2018**, 266, 321.
[19] A. P. Majewski, U. Stahlschmidt, V. Jérôme, R. Freitag, A. H. E. Müller, H. Schmalz, *Biomacromolecules* **2013**, 14, 3081.
[20] R. Chen, M. E. Eccleston, Z. Yue, N. K. H. Slater, *Journal of Materials Chemistry* **2009**, 19, 4217.
[21] G. Kocak, C. Tuncer, V. Bütün, *Polymer Chemistry* **2017**, 8, 144.
[22] M. E. H. El-Sayed, A. S. Hoffman, P. S. Stayton, *Expert Opinion on Biological Therapy* **2005**, 5, 23.
[23] D. W. Pack, A. S. Hoffman, S. Pun, P. S. Stayton, *Nat Rev Drug Discov* **2005**, 4, 581.
[24] P. S. Stayton, M. E. El-Sayed, N. Murthy, V. Bulmus, C. Lackey, C. Cheung, A. S. Hoffman, *Orthod Craniofac Res* **2005**, 8, 219.
[25] S. Zhang, A. Nelson, Z. Coldrick, R. Chen, *Langmuir* **2011**, 27, 8530.
[26] R. Chen, S. Khormaee, M. E. Eccleston, N. K. H. Slater, *Biomaterials* **2009**, 30, 1954.
[27] V. H. Ho, N. K. Slater, R. Chen, *Biomaterials* **2011**, 32, 2953.
[28] S. Khormaee, Y. Choi, M. J. Shen, B. Xu, H. Wu, G. L. Griffiths, R. Chen, N. K. H. Slater, J. K. Park, *Advanced Functional Materials* **2013**, 23, 565.
[29] W. B. Liechty, R. Chen, F. Farzaneh, M. Tavassoli, N. K. H. Slater, *Advanced materials (Deerfield Beach, Fla.)* **2009**, 21, 3910.
[30] A. L. Lynch, R. Chen, P. J. Dominowski, E. Y. Shalaev, R. J. Yancey, Jr., N. K. Slater, *Biomaterials* **2010**, 31, 6096.
[31] A. L. Lynch, R. Chen, N. K. Slater, *Biomaterials* **2011**, 32, 4443.
[32] S. A. Mercado, N. K. H. Slater, *Cryobiology* **2016**, 73, 175.
[33] T. F. Martens, K. Remaut, J. Demeester, S. C. De Smedt, K. Braeckmans, *Nano Today* **2014**, 9, 344.
[34] S. A. Mercado, N. K. H. Slater, *European Polymer Journal* **2016**, 74, 158.
[35] M. Zanoni, F. Piccinini, C. Arienti, A. Zamagni, S. Santi, R. Polico, A. Bevilacqua, A. Tesei, *Scientific reports* **2016**, 6, 19103.
[36] A. Amann, M. Zwierzina, G. Gamerith, M. Bitsche, J. M. Huber, G. F. Vogel, M. Blumer, S. Koeck, E. J. Pechriggl, J. M. Kelm, W. Hilbe, H. Zwierzina, *PloS one* **2014**, 9, e92511.
[37] A. Strasser, H. Puthalakath, P. Bouillet, D. C. Huang, L. O'Connor, L. A. O'Reilly, L. Cullen, S. Cory, J. M. Adams, *Annals of the New York Academy of Sciences* **2000**, 917, 541.

[38] M. F. van Delft, A. H. Wei, K. D. Mason, C. J. Vandenberg, L. Chen, P. E. Czabotar, S. N. Willis, C. L. Scott, C. L. Day, S. Cory, J. M. Adams, A. W. Roberts, D. C. Huang, *Cancer cell* **2006**, 10, 389.
[39] H. Kashiwagi, J. E. McDunn, P. S. Goedegebuure, M. C. Gaffney, K. Chang, K. Trinkaus, D. Piwnica-Worms, R. S. Hotchkiss, W. G. Hawkins, *Annals of Surgical Oncology* **2007**, 14, 1763.
[40] W. T. Godbey, K. K. Wu, A. G. Mikos, *Journal of Biomedical Materials Research* **1999**, 45, 268.
[41] J. W. Wiseman, C. A. Goddard, D. McLelland, W. H. Colledge, *Gene Therapy* **2003**, 10, 1654.
[42] H. Kyung, H. Kim, H. Lee, S. J. Lee, *Journal of Industrial and Engineering Chemistry* **2018**, 58, 290.
[43] A. Erazo-Oliveras, K. Najjar, L. Dayani, T.-Y. Wang, G. A. Johnson, J.-P. Pellois, *Nature Methods* **2014**, 11, 861.
[44] D. Derossi, A. H. Joliot, G. Chassaing, A. Prochiantz, *J Biol Chem* **1994**, 269, 10444.
[45] C. O. Weill, S. Biri, P. Erbacher, *BioTechniques* **2008**, 44, Pvii.
[46] D. Bottger, C. Ullrich, C. Humpel, *Brain research* **2010**, 1312, 108.
[47] S. A. Mercado, C. Orellana-Tavra, A. Chen, N. K. H. Slater, *Materials Science and Engineering: C* **2016**, 69, 1051.
[48] R. Schekman, S. J. Singer, *Proc Natl Acad Sci U S A* **1976**, 73, 4075.
[49] Y. J. Lee, A. Erazo-Oliveras, J. P. Pellois, *Chembiochem: a European journal of chemical biology* **2010**, 11, 325.
[50] J. Z. Gasiorowski, D. A. Dean, *Advanced Drug Delivery Reviews* **2003**, 55, 703.
[51] M. Sui, W. Liu, Y. Shen, *Journal of Controlled Release* **2011**, 155, 227.
[52] L. Li, Z. Y. He, X. W. Wei, G. P. Gao, Y. Q. Wei, *Human gene therapy* **2015**, 26, 452.
[53] H. Kyung, H. Kim, H. Lee, S. J. Lee, *Enhanced Intracellular Delivery of Macromolecules by Melittin Derivatives Mediated Cellular Uptake*, **2018**, 58, 290.

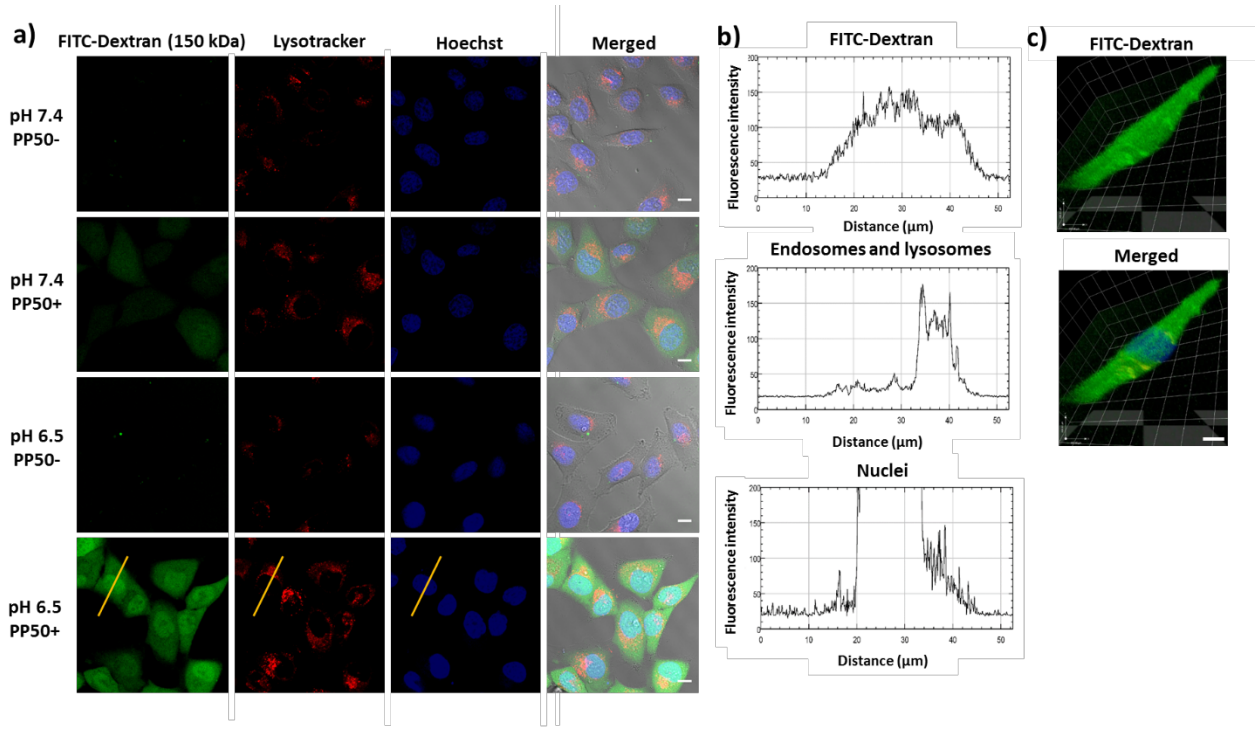

Figure 1. Intracellular delivery using PP50. a) Confocal microscopy illustrating delivery of 150 kDa FITC-Dextran (10 µM) to HeLa cells by co-incubation with PP50 (0.5 mg mL^{-1}) at pH 7.4 and pH 6.5 for a period of 30 min and corresponding polymer-free negative controls (FITC-Dextran only). Scale bar = 10 µm. Yellow line indicates the cross section used to produce the intensity profiles shown in b) with the use of ImageJ. c) 3D projection created using Z-stack obtained via confocal microscopy illustrating the diffused nature of the green fluorescent signal throughout the cytoplasm and the nucleus and the co-localization of the green signal with blue DNA stain Hoechst. Scale bar = 1 µm.

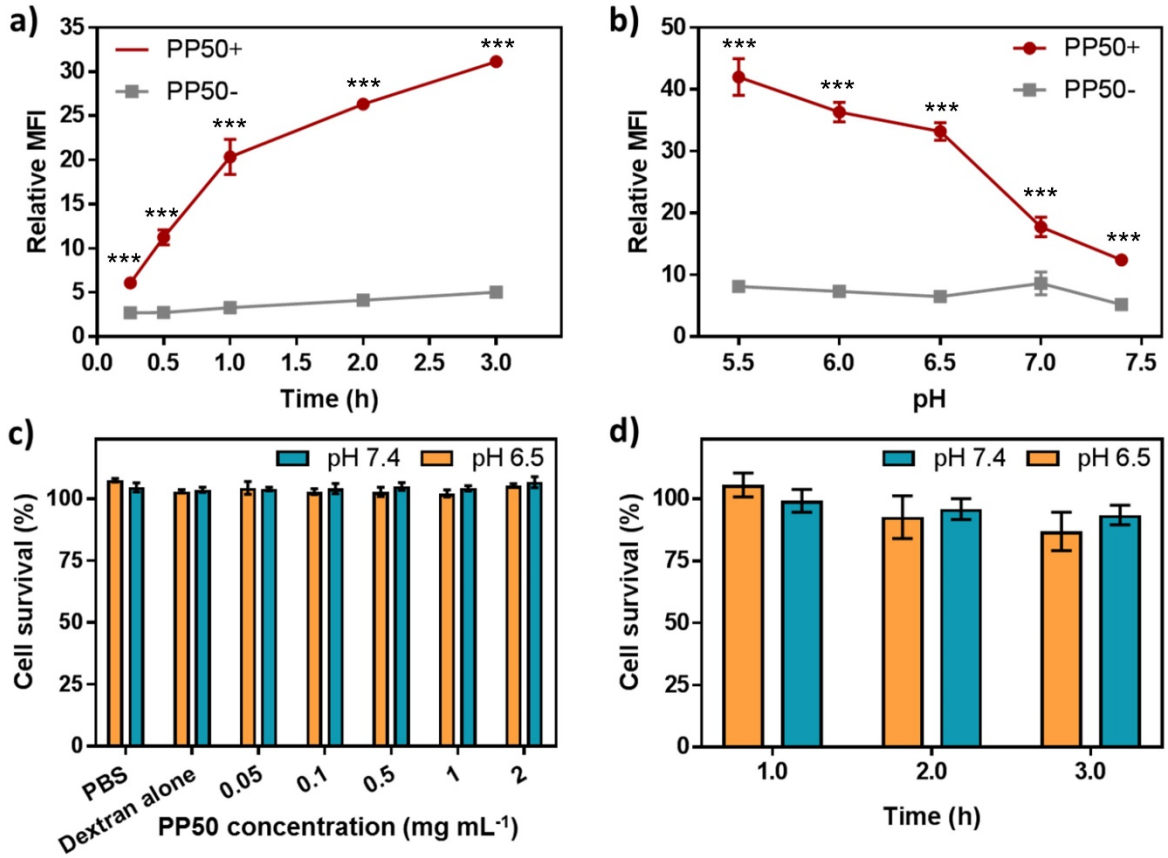

Figure 2. Delivery method characterization using HeLa cells as a model. a) Mean fluorescence intensity (MFI) in HeLa cells after a treatment with a mixture of PP50 (0.5 mg mL^{-1}) and 150 kDa FITC-Dextran (2.5 µM) at pH 6.5 for different time periods within the range of 15-180 min, compared to polymer-free samples. b) The effect of extracellular pH on delivery of 150 kDa FITC-Dextran (5 µM) using PP50 (0.5 mg mL^{-1}). PBS adjusted to pH 5.0-7.4 was used for the treatment time equal to 30 min. Polymer positive and negative samples were compared. c) Cytotoxicity of the delivery process of 150 kDa Dextran (10 µM) after incubation with PP50 (different concentrations used) in PBS for 30 min, determined using AlamarBlue Assay. d) Cytotoxicity of the delivery process determined using AlamarBlue Assay after incubation with PP50 (1 mg mL^{-1}) and 150 kDa Dextran (10 µM) at pH 6.5 and pH 7.4, comparing different treatment times. All samples were analyzed in triplicates (n = 3) and error bars represent mean ± standard deviations. ***$p \leq 0.001$.

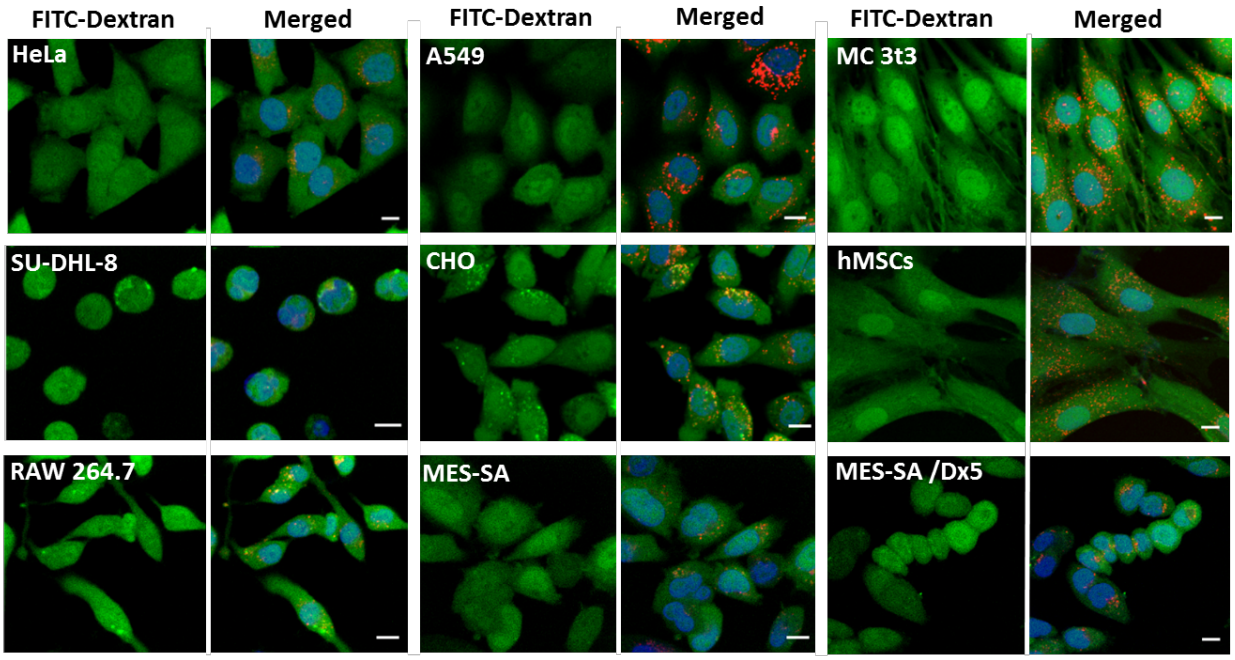

Figure 3. Delivery of 150 kDa FITC-Dextran to different cell lines. Confocal microscopy of 9 different cell lines after delivery of 10 µM FITC-Dextran using 1 mg mL^{-1} PP50 at pH 6.5 in 1 h treatment (HeLa, A549, MC 3t3, SU-DHL-8, CHO, hMSCs) or 5 µM FITC-Dextran in 0.5 h treatment using the same polymer concentration (RAW 264.7, MES-SA, MES-SA/Dx5). Aside from the green channel, the merged pictures contain red (Lysotracker) and blue (Hoechst) channels. Scale bar = 10 µm.

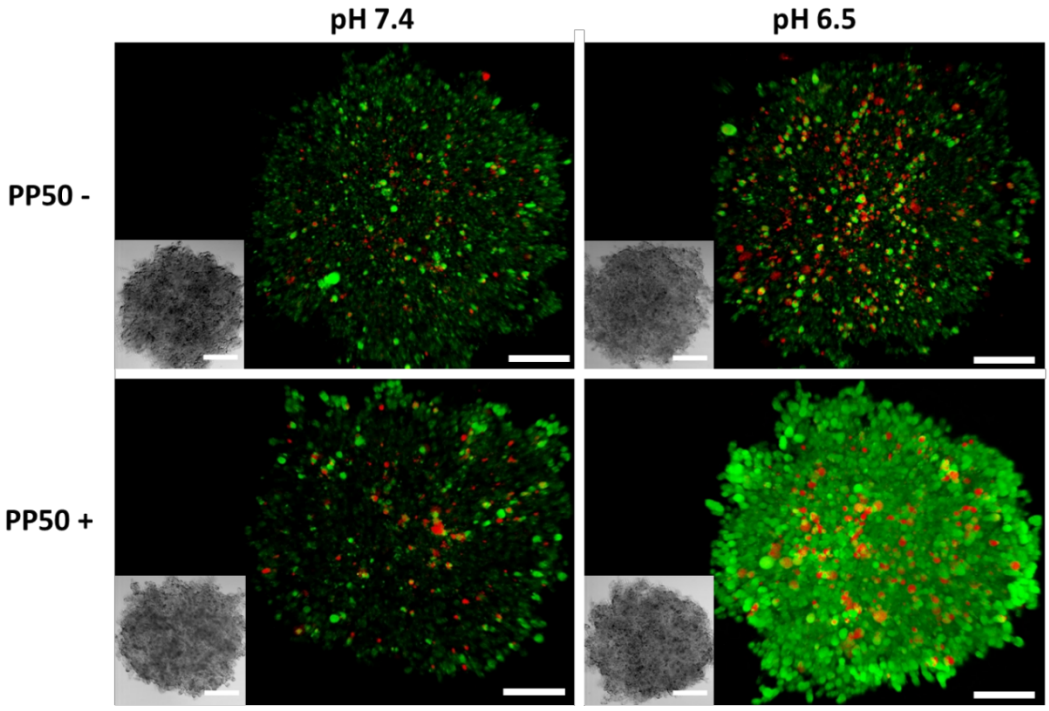

Figure 4. Delivery of 150 kDa FITC-Dextran to A549 human adenocarcinomic alveolar basal epithelial cell spheroids: Z-stacks obtained using confocal microscopy illustrating delivery of FITC-Dextran (10 μM) to the A549 spheroids by co-incubation with PP50 (0.5 mg mL^{-1}) for a period of 2 h. Delivery at pH 6.5 and pH 7.4 was compared, in addition to corresponding polymer-free controls. The 3D projections are shown from the top and are a merge between green channel (FITC-Dextran) and red channel (PI stain of dead cells). The insets show bright field images of the corresponding spheroid. Scale bar = 200 μm.

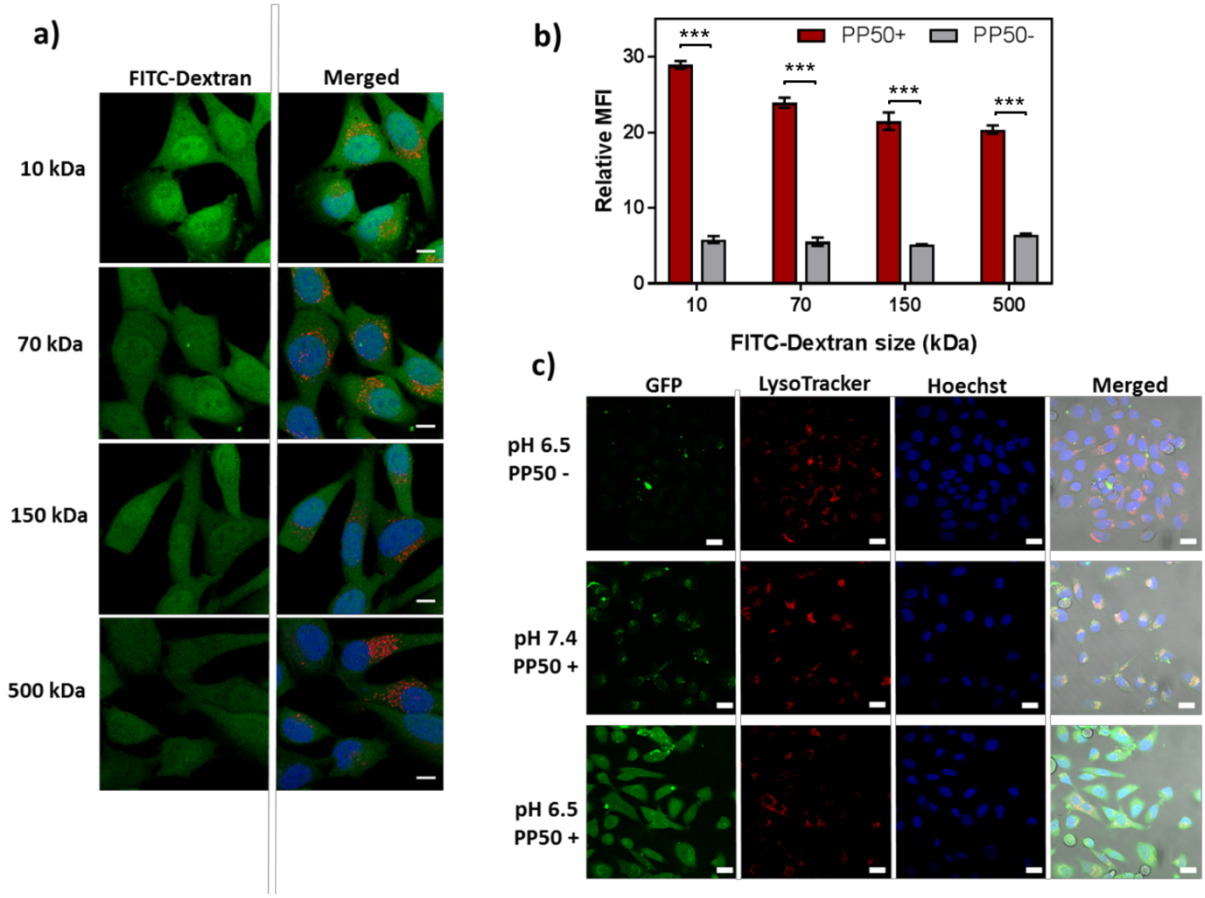

Figure 5. Delivery of different-sized payloads to HeLa cells. a) Confocal microscopy illustrating delivery of 10, 70, 150 and 500 kDa FITC-Dextran (0.15 mg mL^{-1}) using PP50 (0.5 mg mL^{-1}) at pH 6.5 in 30-min treatment. The merged images combine green (FITC-Dextran), red (Lysotracker) and blue (Hoechst) channels. Scale bar = 10 µm. b) Fluorescent signal of cells analyzed by flow cytometry after treatment with PP50 (0.5 mg mL^{-1}) and FITC-Dextran (0.15 mg mL^{-1}) for 1 h. All samples were analyzed in triplicates (n = 3) and error bar represent mean ± standard deviations. c) Delivery of GFP (2 µM) to HeLa cells using PP50 (0.25 mg mL^{-1}) at pH 6.5 and pH 7.4 with 1 h of treatment. Scale bar = 20 µm. ***$p \leq 0.001$.

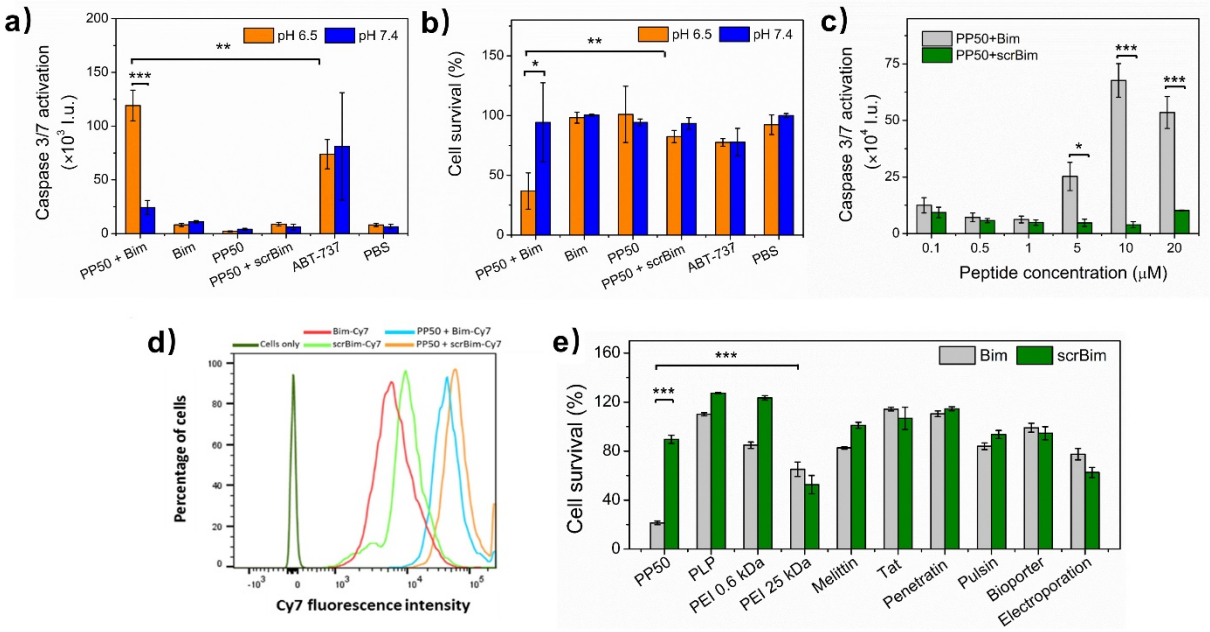

Figure 6. Delivery of Bim peptide to A549 cells. a) Caspase 3/7 activation after delivery of Bim (20 μM) by co-incubation with PP50 (1 mg mL^{-1}) for a period of 3 h at pH 6.5 and pH 7.4, as compared to controls: PP50 mediated delivery of scrambled Bim (scrBim) and cells incubated with Bim, PP50 or PBS alone. Membrane-permeable, small-molecule, Bim-mimetic ABT-737 (20 μM), was used as a positive control. b) Survival of cells treated in the same fashion as in a) after a further incubation period of 24 h, analyzed using AlamarBlue assay. c) Caspase activation after PP50 (0.5 mg mL^{-1})-mediated delivery of Bim and scrBim in the peptide concentration range of 0.1-20 μM at pH 6.5 after 3 h of treatment and 4 h of further incubation. d) Flow cytometry histogram comparing delivery of Cy7-labelled Bim and scrBim (15 μM) using PP50 (1 mg mL^{-1}) at pH 6.5 after 1 h treatment. e) Comparison of the cell death caused by the delivery of Bim-Cy7 (15 μM) using different delivery methods. The treatment time was equal to 4 h for the polymer and peptide-based delivery agents as well as Pulsin® and Bioporter®. Cell survival was quantified using CellTiter-Glo 2.0 assay 24 h after the end of the treatment. All samples were analyzed in triplicates (n = 3) and error bars represent mean ± standard deviations. *$0.01 < p \leq 0.05$; **$0.001 < p \leq 0.01$; and ***$p \leq 0.001$.

Table 1. A selection of physical, chemical and biological delivery methods for intracellular delivery of various materials

Method	Characteristics	Reference
	Physical	
Electroporation	(+) Delivery of DNA, RNA and protein into a wide range of cells (–) High cellular toxicity	[9, 10]
Cell squeezing	(+) Delivery of a wide range of payloads to different types of detached cells (–) Limited throughput due to clogging (–) Potential problems with scalability (–) Inability to deliver to cells grown as adherent cultures, multicellular aggregates, or tissues	[11, 12]
	Chemical and biological	
Viral vectors	(+) Good transfection efficiency (–) Limited *in vivo* due to safety concerns and production difficulties	[4]
Exosomes and liposomes	(+) Good potential for *in vivo* delivery (+) Compatible with hydrophilic and hydrophobic payloads and various cell types (–) Preparation techniques are complex and laborious (–) Require additional steps for encapsulation of the desired payloads	[13, 14]
CPPs	(+) Overcome the problem of endosomal entrapment for delivery of different payloads to various cell types (–) Low efficiency (–) Costly synthesis and low scalability	[15 – 17]
Cationic pH-responsive polymers	(+) Allow gene delivery (+) Interact with the negatively charged plasma membrane (–) Potential problems with high cytotoxicity	[18, 19]
Anionic pH-responsive polymers	(+) Enable *in vivo* and *in vitro* delivery of various payloads (+) Low cytotoxicity (–) Electrostatic repulsion from the negatively charged membrane and nucleic acid payloads	[20 – 22]